Proceedings of the 28th IEEE
EMBS Annual International Conference
New York City, USA, Aug 30-Sept 3, 2006

An Implementation of Image Sharpening Based on Morphological Operations for Ubiquitous Echo

Masayoshi Tsubai, Naoshi Mitoda, Osamu Fukuda, and Naohiro Ueno

Abstract— **Ubiquitous Echo is a portable ultrasound imaging equipment. We discuss an image sharpening method based on geometrical information by mathematical morphology with double structuring element (DSE) for on-line processing on Ubiquitous Echo. The sharpening method improves the contrast of tissue boundaries without speckle emphasis. The computational complexity of the morphological operations is reduced by chain rule of the operations and decomposition of the DSE not to delay refreshing the ultrasound moving image.**

I. Introduction

We implement an edge sharpening based on morphological operations with double structuring element (DSE) for ultrasound moving image of Ubiquitous Echo. To reduce computational complexity of the morphological operations, usually, chain rule of the operations and decomposition of the structuring element are applied. In the case of the morphological operations using DSE, however, it seems that the chain rule cannot be applied. The reason is that the DSE cannot be decomposed since the gray values of the DSE are not constant within its domain. In this paper, we introduce the chain rule into the morphological operation using DSE. The computational complexity of the morphological operations is reduced by chain rule of the operations and decomposition of the DSE not to delay refreshing the ultrasound moving image of the Ubiquitous Echo.

Ubiquitous Echo is a portable ultrasound imaging equipment which is small, lightweight, and inexpensive. The unit was developed through joint research between the National Institute of Advanced Industrial Science and Technology (AIST) and the Hiroshima Institute of Technology. The unit can be used in health care or beauty facilities, or even in the home, to visualize components of the body such as muscles, bones, and subcutaneous fat. Users connect Ubiquitous Echo to their personal computers and use the included software to collect detailed information about specific parts of the body. The ultrasonic diagnostic equipment traditionally used in medical examinations is prohibitively expensive and too large to be used by health care and beauty facilities or in the home.

This work was supported in part by Grant-in-Aid for Young Scientists (B) (No. 17700407) from the Ministry of Education, Science, Sports and Culture.

M. Tsubai, O. Fukuda, and N. Ueno are with On-site Sensing and Diagnosis Research Laboratory, National Institute of Advanced Industrial Science and Technology (AIST), 807-1 Shuku-machi, Tosu, Saga 841-0052, Japan

N. Mitoda is with the ISLabo, Co., Ltd., Japan

Generally, edge sharpening or contrast enhancement can be realized by emphasizing high frequency contents of the image [3]–[5]. However, noise also includes much high frequency contents. It is difficult to suppress the noise emphasis while the edge is sharpened. Furthermore, overshoot and undershoot occur at top and bottom of the edge slope, respectively. It may be effective to recognize the enhanced edge by human eyes. However, it is not desirable for diagnosis and analysis, because overshoot and undershoot may be confused with some original edges. For example, a roof-like edge and an overshooting step-like edge are confused.

As the other approaches for edge sharpening, the shock filter [6] and a morphological method by switching results of dilation and erosion [7] are proposed. These methods can restore a blurred step edge without noise to an ideal step edge without overshoot nor undershoot. However, these methods are sensitive to noise and distortion of the input image. In the ultrasound image, due to the sensitivity, speckles are emphasized significantly.

Anisotropic diffusion was proposed for noise reduction and edge enhancement [8], [9]. It was applied to ultrasound images for speckle reduction [10], [11]. The anisotropic diffusion can enhance edges and reduce noises simultaneously, however, it cannot sharpen edges without smoothing.

We proposed a morphological edge sharpening by DSE and applied it to edge sharpening of ultrasound images [2]. The morphological edge sharpening resolved the problems. The proposed method improved the contrast of brightness around the tissue boundary without speckle emphasis, overshoot nor undershoot.

The DSE is a pair of two different structuring elements. Important factors of the DSE are its domain and gray values. The gray values of the DSE are controlled spatially to sharpen edges of the image components. The opening operation of an input image by DSE eliminates image components whose support does not cover the DSE, and sharpens edges of the image components which can contain the DSE.

As the other study of morphological operations, adaptive morphological operations were proposed for noise reduction [12]–[16]. The concept of the adaptive morphological operations is to remove noises while preserving features by changing the domain of the structuring element with respect to spatial positions. The domain is changed to adapt its shape and size for local structures. The adaptive morphological operations do not yield the edge sharpening which the DSE yields.

The sharpening method based on morphological operations with DSE showed better performance in sharpening edges of the ultrasound images while speckles are kept from being emphasized compared with several sharpening methods based on unsharp masking [1], [2]. The morphological edge sharpening was evaluated quantitatively using detail variance(DV) and background variance(BV) [1]. The DV is variance of the gray values within the region which covers the boundary, and the BV is variance of the gray values within the region which does not contain the boundary [4]. The morphological edge sharpening enlarged the DV of the images while the BV was kept sufficiently small, but the unsharp masking enlarged both the DV and the BV.

In this paper, we introduce a fast computation of the morphological edge sharpening for Ubiquitous Echo. The computational complexity of the morphological operations with DSE is reduced by chain rule of the operations and decomposition of the DSE. Our experimental result shows that the proposed sharpening method little reduces the frame rate of the Ubiquitous Echo.

II. Gray-scale morphology using double structuring element

A. Definitions of morphological operations

Let f, $f : F \to E$, $F \subseteq E^{N-1}$ be an input gray-scale image. E^{N-1} means Euclidean (N-1)-space. Let $g_{\boldsymbol{x}}$, $g_{\boldsymbol{x}} : G \to E$ be a spatially variant structuring element with respect to the position $\boldsymbol{x}$, where $G \subseteq E^{N-1}$ is domain of $g_{\boldsymbol{x}}$. Let $\mathbf{g} = \{g_{\boldsymbol{x}} | \boldsymbol{x} \in F\}$. Let the domain of $g_{\boldsymbol{x}}$, G, be spatially invariant to simplify the calculation and reduce computational complexity.

The space-varying erosion of f by $\mathbf{g}$, dilation of f by $\mathbf{g}$, and opening of f by $\mathbf{g}$ are defined as [14]

$$(f \ominus \mathbf{g})(\boldsymbol{x}) = \min_{\boldsymbol{z} \in G} \{f(\boldsymbol{x}+\boldsymbol{z}) - g_{\boldsymbol{x}}(\boldsymbol{z})\}, \quad (1)$$

$$(f \oplus \mathbf{g})(\boldsymbol{x}) = \max_{\boldsymbol{z} \in G} \{f(\boldsymbol{x}-\boldsymbol{z}) + g_{\boldsymbol{x}-\boldsymbol{z}}(\boldsymbol{z})\}, \quad (2)$$

$$f \circ \mathbf{g} = (f \ominus \mathbf{g}) \oplus \mathbf{g}. \quad (3)$$

Let $\dot{g}_{\boldsymbol{x}}$, $\dot{g}_{\boldsymbol{x}} : G \to E$ be another spatially variant structuring element with respect to the position $\boldsymbol{x}$. Let $g_{\boldsymbol{x}} \geq \dot{g}_{\boldsymbol{x}}$ and $\dot{\mathbf{g}} = \{\dot{g}_{\boldsymbol{x}} | \boldsymbol{x} \in F\}$. A pair of two structuring elements $g_{\boldsymbol{x}}$ and $\dot{g}_{\boldsymbol{x}}$, denoted by $(\mathbf{g}, \dot{\mathbf{g}})$, is named as double structuring element (DSE) [2].

The opening of f by DSEs $(\mathbf{g}, \dot{\mathbf{g}})$, denoted by $f \circ (\mathbf{g}, \dot{\mathbf{g}})$, is defined as [2]

$$f \circ (\mathbf{g}, \dot{\mathbf{g}}) = (f \ominus \mathbf{g}) \oplus \dot{\mathbf{g}}. \quad (4)$$

The closing of f by $(\mathbf{g}, \dot{\mathbf{g}})$, which is dual operation for the opening, denoted by $f \bullet (\mathbf{g}, \dot{\mathbf{g}})$, is defined as

$$f \bullet (\mathbf{g}, \dot{\mathbf{g}}) = -[(-f) \circ (\mathbf{g}^s, \dot{\mathbf{g}}^s)], \quad (5)$$

where superscript s means reflection. The reflection of $g_{\boldsymbol{x}} : G \to E$ is defined by $g^s_{\boldsymbol{x}} : G^s \to E$, $g^s_{\boldsymbol{x}}(\boldsymbol{z}) = g_{\boldsymbol{x}}(-\boldsymbol{z})$, $G^s_{\boldsymbol{x}} = \{b \mid b = -a, a \in G\}$.

B. Edge sharpening operation

The result f_e of edge sharpening operation of an image f is obtained from opening and closing as [2]

$$f_e = f + f \circ (\mathbf{g}, \dot{\mathbf{g}}) - f \circ \mathbf{g} + f \bullet (\mathbf{g}^s, \dot{\mathbf{g}}^s) - f \bullet \mathbf{g}^s. \quad (6)$$

Correction terms added to f in the right-hand side of (6) are edge-sharpening components, which are extracted from opening processes and closing processes. The corrections in (6) sharpen edges of the image components which can contain the DSEs. Image components whose support does not cover the DSEs are preserved.

For ultrasound image processing, in order not to sharpen speckles, domain of the DSE should be large enough to cover support of the speckle cell. Furthermore, it should be kept sufficiently small for accurate sharpening in fine structures.

C. Gray value of the DSE

In order to make the opening by DSEs yield edge sharpening, gray values of the DSE are determined as follows. A function $c : F \to E$ is prepared to control the gray values of the DSE. Assume that c satisfies following two conditions: (a) c has maximum value at the boundary, and (b) c is constant in homogeneous regions without boundary. The gray values of the DSE are controlled under the function c as [2]

$$g_{\boldsymbol{x}}(\boldsymbol{z}) = \begin{cases} 0 & \text{if } \boldsymbol{z} \in G, \\ -\infty & \text{otherwise.} \end{cases} \quad (7)$$

$$\dot{g}_{\boldsymbol{x}}(\boldsymbol{z}) = \begin{cases} \min_{\boldsymbol{u} \in G} c(\boldsymbol{x}-\boldsymbol{u}+\boldsymbol{z}) - c(\boldsymbol{x}) & \text{if } \boldsymbol{z} \in G, \\ -\infty & \text{otherwise.} \end{cases} \quad (8)$$

The function c, which reflects a local information of the input image f, is obtained as

$$c(\boldsymbol{x}) = \alpha \Big\{ \max_{\boldsymbol{u} \in G_{\boldsymbol{x}}} f(\boldsymbol{x}+\boldsymbol{u}) - \min_{\boldsymbol{u} \in G_{\boldsymbol{x}}} f(\boldsymbol{x}+\boldsymbol{u}) \Big\}, \quad (9)$$

where α is positive coefficient which adjusts sharpness of the output image. The sharpness of the image increases with an increase in α. The control $c(\boldsymbol{x})$ is obtained as a difference of local maximum and local minimum around a spatial position $\boldsymbol{x}$ of the input image $f(\boldsymbol{x})$. The difference reflects edges of the input image.

III. Reduction of computational complexity

Computational complexity of the morphological operations is proportional to the number of pixels within the structuring element. To reduce computational complexity of the morphological operations, chain rule of the operations and decomposition of the structuring element are used well.

The structuring element $g_{\boldsymbol{x}}$ in (7) is easy to be decomposable since its gray values $g_{\boldsymbol{x}}(\boldsymbol{z})$ are constant. However, the $\dot{g_{\boldsymbol{x}}}$ in (8) does not seem to be decomposable since its gray values $\dot{g_{\boldsymbol{x}}}(\boldsymbol{z})$ are not fixed within its domain G.

As the following procedure, the $\dot{g_{\boldsymbol{x}}}$ can be eliminated from (4). First, in (8), we replace $\boldsymbol{x}$ by $\boldsymbol{x}-\boldsymbol{z}$ as

$$\dot{g}_{\boldsymbol{x}-\boldsymbol{z}}(\boldsymbol{z}) = \min_{\boldsymbol{u}\in G} \ c(\boldsymbol{x}-\boldsymbol{u}) - c(\boldsymbol{x}-\boldsymbol{z}). \tag{10}$$

From (4),

$$\begin{aligned}
&[f \circ (\mathbf{g}, \dot{\mathbf{g}})](\boldsymbol{x}) \\
&\quad = \max_{\boldsymbol{z}\in G} \{(f \ominus \mathbf{g})(\boldsymbol{x}-\boldsymbol{z}) + \dot{g}_{\boldsymbol{x}-\boldsymbol{z}}(\boldsymbol{z})\} \\
&\quad = \max_{\boldsymbol{z}\in G} \left\{(f \ominus \mathbf{g})(\boldsymbol{x}-\boldsymbol{z}) + \min_{\boldsymbol{u}\in G} c(\boldsymbol{x}-\boldsymbol{u}) - c(\boldsymbol{x}-\boldsymbol{z})\right\} \\
&\quad = \max_{\boldsymbol{z}\in G} \{(f \ominus \mathbf{g})(\boldsymbol{x}-\boldsymbol{z}) - c(\boldsymbol{x}-\boldsymbol{z})\} + \min_{\boldsymbol{u}\in G} c(\boldsymbol{x}-\boldsymbol{u}) \\
&\quad = \max_{\boldsymbol{z}\in G} \{(f \ominus \mathbf{g})(\boldsymbol{x}-\boldsymbol{z}) - c(\boldsymbol{x}-\boldsymbol{z})\} - \max_{\boldsymbol{z}\in G} \{-c(\boldsymbol{x}-\boldsymbol{z})\}.
\end{aligned} \tag{11}$$

By using (2) and (7), we get

$$f \circ (\mathbf{g}, \dot{\mathbf{g}}) = (f \ominus \mathbf{g} - c) \oplus \mathbf{g} \, - \, (-c) \oplus \mathbf{g}. \tag{12}$$

Similarly, the closing is expressed as

$$f \bullet (\mathbf{g}, \dot{\mathbf{g}}) = \, - \{ \, (-f) \ominus \mathbf{g}^s - c \, \} \oplus \mathbf{g}^s \, + \, (-c) \oplus \mathbf{g}^s. \tag{13}$$

Since $g_{\boldsymbol{x}}$ and $g^s_{\boldsymbol{x}}$ are spatially invariant as shown in (7), (13) is rewritten using duality between erosion and dilation expressed by $(-f) \ominus \mathbf{g}^s = -f \oplus \mathbf{g}$ and $(-f) \oplus \mathbf{g}^s = -f \ominus \mathbf{g}$ as

$$f \bullet (\mathbf{g}, \dot{\mathbf{g}}) = (f \oplus \mathbf{g} + c) \ominus \mathbf{g} + (-c) \oplus \mathbf{g}^s. \tag{14}$$

Edge sharpening operation in (6) can be expressed using (12) and (14) as

$$\begin{aligned} f_e = f &+ (f \ominus \mathbf{g} - c) \oplus \mathbf{g} - (f \ominus \mathbf{g}) \oplus \mathbf{g} \\ &+ (f \oplus \mathbf{g}^s + c) \ominus \mathbf{g}^s - (f \oplus \mathbf{g}^s) \ominus \mathbf{g}^s. \end{aligned} \tag{15}$$

IV. Application to Ubiquitous Echo

A. Implementation for Ubiquitous Echo

The Ubiquitous Echo outputs 2-dimensional gray scale images. As a decomposable DSE, we use a 2-dimensional rectangular domain of the structuring element, denoted by b_s, whose horizontal width is M and vertical width is N.

From (15), edge sharpening operation becomes

$$\begin{aligned} f_e = f &+ (f \ominus b_s - c) \oplus b_s - (f \ominus b_s) \oplus b_s \\ &+ (f \oplus b_s + c) \ominus b_s - (f \oplus b_s) \ominus b_s. \end{aligned} \tag{16}$$

The function c, from (9), is expressed as

$$c = \alpha(f \oplus b_s - f \ominus b_s). \tag{17}$$

The rectangular domain is decomposable into orthogonal two linear structuring elements. One is M pixels of a horizontal structuring element b_h, and another is N pixels of a vertical structuring element b_v. The rectangular structuring element is expressed through morphological dilation as $b_s = b_h \oplus b_v$.

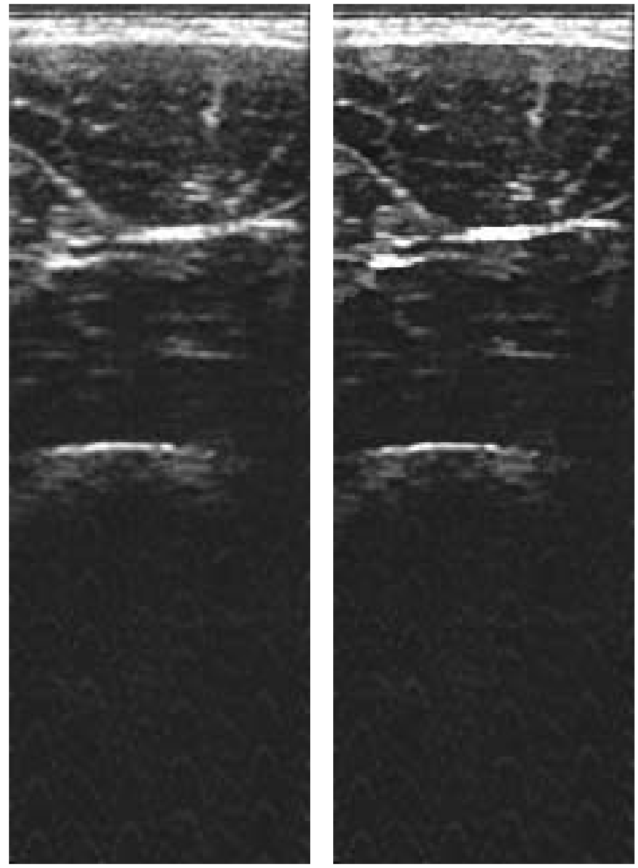

(a) (b)

Fig. 1. Edge sharpening result of an ultrasound femoral image. (a) Original image. (b) Sharpened image.

The erosion of f by b_s and the dilation of f by b_s can be computed using chain rule as

$$f \ominus b_s = (f \ominus b_h) \ominus b_v, \tag{18}$$
$$f \oplus b_s = (f \oplus b_h) \oplus b_v. \tag{19}$$

The computational complexity is reduced from $M \times N$ to $M + N$.

B. Experimental results

The Ubiquitous Echo outputs 2-dimensional gray scale moving image of 122×320 pixels and 256 gray levels. The image is transferred online to a computer, and the image is drawn on a display of the computer. The frame rate depends on performance of the computer. In the experiment, we connected the Ubiquitous Echo to a laptop computer whose CPU was Intel Pentium M 1.2GHz. Frame rate of the moving image without edge sharpening was 6.4 frames/s.

The software for edge sharpening operation was executed on the laptop computer. Figure 1(a) shows a human femoral image acquired by Ubiquitous Echo. The edge sharpening result is shown in Fig.1(b). Boundaries of muscle, fat and bone are sharpened while speckles are not emphasized and details are preserved. Frame rate of the moving image with

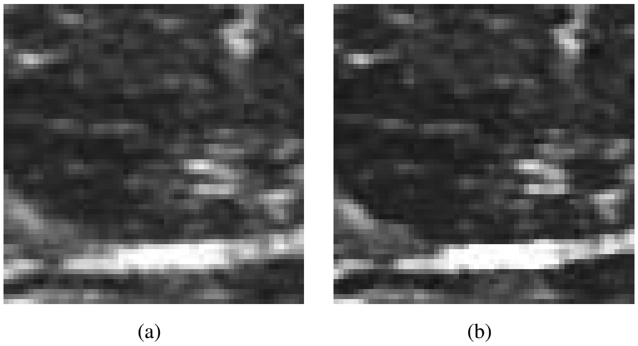

Fig. 2. Enlarged images of the edge sharpening result. (a) Original image. (b) Sharpened image.

edge sharpening was 5.8 frames/s. Original frame rate was almost kept.

Figure 2 shows enlarged images around a boundary between muscles. The sharpened image are deblurred around the boundary and in the detail. Speckles in the sharpened image are almost identical with the original.

The parameters used for enhancement process were chosen as $M = 9$, $N = 5$, and $\alpha = 1.0$. M and N were determined as 3 times of speckle cell size so that supports of the speckle cells are covered by the domain of the DSE. If α = 0, then processed image is identical with the original image. If α is sufficiently large, then the image is fully sharpened but it may be artificial. Our experimental result [1] shows that the sharpness was almost saturated at α = 10. Therefore, the α was chosen experimentally between 0 and 10 in terms both of sharpness and of naturalness of the processed image.

V. Conclusions

We implemented an image sharpening method based on morphological operations with double structuring element for on-line processing on Ubiquitous Echo. Original frame rate of the moving image was almost kept under the on-line processing. The sharpening method improved the contrast of tissue boundaries without speckle emphasis. The computational complexity of the morphological operations was reduced by chain rule of the operations and decomposition of the double structuring element.

References

[1] M. Tsubai, and M. Ito, "Edge enhancement of ultrasonic images by morphological operations based on locally variable structuring elements," *IEICE Trans. Information and Systems*, vol. 85-D, no. 1, pp. 190–198, 2002.

[2] M. Tsubai, T. Nishimura, A. Sasaki, T. Mitake, and S. Umemura, "A study of morphological edge enhancement by double structuring element for ultrasound B-mode images," *Proc. 2004 IEEE Ultrasonics Symposium*, pp. 1437–1440, 2004.

[3] F. Neycenssac, "Contrast enhancement using the Laplacian-of-a-Gaussian filter," *CVGIP: Graphic. Model. Image Process.*, Vol. 55, No. 6, pp. 447–463, 1993.

[4] G. Ramponi, "A cubic unsharp masking technique for contrast enhancement," *Signal Process.*, vol. 67, no. 2, pp. 211–222, 1998.

[5] A. Polesel, G. Ramponi, and V. J. Mathews, "Image enhancement via adaptive unsharp masking," *IEEE Trans. Image Process.*, vol. 9, no. 3, pp. 505–510, 2000.

[6] S. Osher, and L. I. Fudin, "Feature-oriented image enhancement using shock filter," *SIAM J. Numerical Analysis.*, vol. 27, pp. 919–940, 1990.

[7] J. G. M. Schavemaker, M. J. T. Reinders, J. J. Gerbrands, and E. Backer, "Image sharpening by morphological filtering," *Pattern Recogn.*, vol. 33, pp. 997–1012, 2000.

[8] P. Perona, and J. Malik, "Scale-space and edge detection using anisotropic diffusion," *IEEE Trans. Pattern Anal. Machine Intell.*, vol. 12, no. 7, pp. 629–639, 1990.

[9] M. J. Black, and G. Sapiro, "Robust anisotropic diffusion," *IEEE Trans. Image Process.*, vol. 7, no. 3, pp. 421–432, 1998.

[10] K. Z. Abd-Elmoniem, A. M. Youssef, and Y. M. Kadah, "Real-time speckle reduction and coherence enhancement in ultrasound imaging via nonlinear anisotropic diffusion," *IEEE Trans. Biomed. Eng.*, vol. 49, no. 9, pp. 997–1014, 2002.

[11] J. Montagnat, M. Sermesant, H. Delingette, G. Malandain, and N. Ayache, "Anisotropic filtering for model-based segmentation of 4D cylindrical echocardiographic images," *Pattern Recogn. Letters*, vol. 24, pp. 815–828, 2003.

[12] J. Song, and E. J. Delp, "The analysis of morphological filters with multiple structuring elements," *Comput. Vision Graphics Image Process.*, vol. 50, pp. 308–328, 1990.

[13] F. Cheng, and A. N. Venetsanopoulos, "An adaptive morphological filter for image processing," *IEEE Trans. on Image Processing*, vol. 1, pp. 533–539, 1992.

[14] C. S. Chen, J. L. Wu, and Y. P. Hung, "Statistical analysis of space-varying morphological openings with flat structuring elements," *IEEE Trans. on Signal Process.*, vol. 44, no. 4, pp. 1010–1014, 1996.

[15] C. S. Chen, J. L. Wu, and Y. P. Hung, "Theoretical aspects of vertically invariant gray-level morphological operators and their application on adaptive signal and image filtering," *IEEE Trans. on Signal Process.*, vol. 47, no. 4, pp. 1049–1060, 1999.

[16] F. Cheng, and A. N. Venetsanopoulos, "Adaptive morphological operations, fast algorithms and their applications," *Pattern Recogn.*, vol. 33, pp. 917–933, 2000.

[17] M. C. Chefchaouni, and D. Schonfeld, "Spatially-variant mathematical morphology," *Proc. ICIP-94*, vol. 2, pp. 555–559, 1994.